PHASE BEHAVIOR OF SEVERAL CO_2 WEST TEXAS RESERVOIR OIL SYSTEMS

EDWARD A. TUREK, ROBERT S. METCALFE and
ROBERT E. FISHBACK
Amoco Production Company

INTRODUCTION

Current interest in miscible enhanced oil recovery methods has led to the use of compositional simulators to understand and predict the performance of such processes. Fluid property considerations are highly important from two standpoints:

1. An essential part of such a simulator is a means of predicting the complex phase equilibria likely to be encountered in such EOR processes. While reliable equations of state have been developed to calculate phase behavior in these processes, most often parameter adjustments are required to properly describe the CO_2-reservoir oil systems. These adjustments require experimental data on systems of interest.

2. The evaluation of the physics required in such a simulator depends upon an understanding of the fluid properties that will be encountered. The relative importance of viscous fingering, gravity override, physical dispersion and low interfacial tension effects must be assessed through interpretation of laboratory CO_2 coreflood and pilot field studies. This requires an understanding of the phase equilibria encountered in such processes and the ability to make reliable predictions.

For these reasons, an experimental study of the phase behavior exhibited by CO_2-West Texas reservoir oil systems was initiated. The resulting data serve as criteria for the evaluation of predictive tools and to advance the general understanding of fluid properties encountered in these systems. With the exception of compositional analyses, which are tabulated in this paper, fluid properties measured in this work are presented graphically; however, values can be read from the figures generally to the accuracy that the properties were measured.

MEASUREMENT PROCEDURE

Both static (single-contact) and multiple contact phase equilibria measurements have been conducted for mixtures of CO_2 with various West Texas reservoir oils. Static tests were performed to accurately define phase boundaries and quality (volume percent oil-rich phase) lines, to determine equilibrium phase compositions and to measure phase densities and viscosities. Multiple contact measurements provided phase splits, equilibrium phase compositions, phase densities and phase viscosities as bulk hydrocarbon compositions were altered through the oil cycling and CO_2 cycling processes.

Following the laboratory procedures developed by Jacoby and Yarborough,[1] each reservoir oil was prepared by recombination of primary separator liquid and gas to agree with the compositions and bubble point pressures determined for the previously studied oils from these fields. Analyses of the recombined reservoir oils are shown

Originally presented as SPE 13117 at the 59th Ann. Tech. Conf. & Exhib., Houston, Tx., Sept. 16-19, 1984. Copyright held by SPE.

in Table 1. Breakdowns of the C_7+ fractions are given in terms of narrow boiling point cuts centered around the boiling points of the normal paraffin components. Specific gravities and molecular weights are also listed for the lumped C_7+ heavy ends. Also included are weathered oil samples used to assess the effects of using "dead" oils in the phase equilibria studies. Recombined oil was weathered by placing an open beaker of the oil on a stirred heating plate within an exhaust hood for 24 hours at the specified temperature.

Static Phase Equilibria Measurements

Static phase equilibria measurements were conducted in the following manner. Each recombined reservoir oil was charged to the variable volume windowed PVT cell[2] in which the phase equilibria measurements were performed. CO_2 was then added incrementally to obtain the desired mixture compositions. Pressure was continually increased until a single-phase condition was observed. The fluids were continually agitated during these steps to insure homogeneity of the single-phase fluid. A constant temperature pressure-volume traverse was then performed to establish the saturation pressure of the mixture and to check for the presence of three phases (oil-rich liquid, CO_2-rich liquid and vapor) at high bulk CO_2 compositions. Sufficient time for mixing and equilibration was allowed between each pressure reduction to insure stable conditions. Mixtures of the reservoir oil and CO_2 led to the precipitation of a finely dispersed asphaltic phase. This phase did not settle out appreciably with time (up to 48 hours) but in some cases did obscure visual observation of the cell contents. Its presence was disregarded with respect to our conclusions concerning the attainment of equilibrium. (Its presence was also discounted with regard to phase volumes.) If three phases were observed, the upper and lower pressure bounds were located. These steps were repeated until the three-phase locus was established in overall composition space at a given temperature. Phase compositions were determined by chromatographic analysis using dimple valves[2] to trap fluid samples from the equilibrium cell and introduce them directly in the carrier gas stream of the temperature programmed chromatograph. Molecular weights were determined by cryoscopic freezing point depression. Phase densities were measured in high pressure pycnometers and phase viscosities were measured in a rolling ball viscometer. Phase volume measurements were performed visually and overall material balances were calculated for the cell contents to test the consistency of the density measurements.

Cycling Studies

CO_2 cycling studies were performed with Oils A, B1, C1 and F for the purpose of simulating the multiple contact phase equilibria experienced by residual oil within a reservoir during a CO_2 flood. CO_2 cycling was conducted in the following manner. Recombined reservoir oil was charged to the variable volume fluid property cell. CO_2 was added incrementally until a composition in the liquid-liquid region was attained. Following equilibration at a fixed pressure and sampling of the phases, the CO_2-rich liquid phase was removed from the cell while the pressure was maintained by reducing the cell volume. Additional CO_2 was then charged to the cell and the system was allowed to equilibrate. The phases present at this point are labeled "second CO_2 contact" within this paper. Following the sampling of these phases for density, viscosity and compositional measurements, the CO_2-rich liquid phase was again removed from the cell at constant pressure. Additional CO_2 was charged to create "third contact" phase equilibria.

Oil cycling studies were conducted on the CO_2-Oil A system and the CO_2-Oil B1 oil system to simulate the multiple contact phase equilibria at the CO_2 flood front. These studies consisted of the following operations. First, pure CO_2 was charged to the fluid property cell. Sufficient recombined reservoir oil was charged to give a bulk composition of approximately 90 mole% CO_2. Equilibrium was attained and the phases were sampled. At constant pressure, the oil-rich liquid phase was then removed from the cell. A second charge of recombined oil of the same volume as the first was added. After attaining equilibrium and sampling the phases, the oil-rich liquid phase was again discarded and a third recombined oil charge was added. After equilibrating, the phases were again sampled to measure density, viscosity, and composition. Additional oil cycles were performed for the CO_2-Oil B1 oil study.

RESULTS

The measurements reported here were conducted over the past five years, during which time analytical techniques and fluid property equipment configurations have evolved. Some trends apparent in the data represent refinement of technique rather than actual differences among the systems studied. The authors have attempted to provide our best estimates of compositions and properties subject to reinterpretation as the better techniques evolved. We believe our results are subject to the following uncertainties. Compositional analyses represent average analyses selected from several replicates in most cases. This selection procedure is necessary to eliminate analytic errors in some cases as large as ±5 mole% for major components. Following the selection procedure, analyses reported here are estimated to be accurate to ±1 mole percent for major components. Uncertainties in gas chromatography measurements were discussed in detail by Yarborough.[3] Some unexpected differences in C_7+ detailed breakdowns were measured for wells in the same field. We attribute this primarily to analytic error and recommend that C_7+ distributions be averaged over a given formation before use. Measured bubble point pressures are generally good to ±5 psi [±37 kPa]. Three-phase boundaries are more difficult to determine due to the opacity of the reservoir oils and their asphaltic precipitates. The reported boundaries are generally reliable to ±25 psi [±170 kPa]. Volumetric phase distribution data suffer from the same visual problems and are believed to be accurate to ±5 vol%. Phase density measurements involving the use of pycnometers encounter problems associated with single-phase fluid transfer and with the determination of small mass changes in a relatively heavy object. Reported densities are normally good to ±0.005 g/cc [5 kg/m^3]. Phase viscosities are generally reproducible to ±10% for viscosities greater than 0.5 cp [0.0005 Pa-s] and ±50% for values less than 0.5 cp but these are highly sensitive to the recombined oil composition. The high uncertainty in low viscosity values reflect the limits of the rolling ball apparatus used in this work. C_7+ properties depend upon fractionation reproducibility and our ability to measure specific gravities and cryoscopic molecular weights. C_7+ specific gravities are believed to be accurate to ±0.3% and C_7+ molecular weights are estimated accurate to ±5%.

Static Measurements

Static phase equilibrium measurements for the CO_2-West Texas oil systems described above are presented in terms of pressure-composition phase diagrams (Figures 1-11), equilibrium phase compositions (Tables 2 and 3), phase densities (Figures 12 and 13) and phase viscosities (Figures 14 and 15). Several general observations apply to all systems. For bulk CO_2 compositions below approximately 60 mole%, these systems exhibit conventional bubble point behavior as illustrated by the phase boundaries plotted in Figures 1-11. For bulk CO_2 compositions in excess of 70 mole% for those systems studied at or below 110°F [316.5 K] and at elevated pressures, a CO_2-rich liquid (labeled "L_2" in the figures) coexists with the oil-rich liquid (labeled "L_1") which was present at lower CO_2 compositions. At high CO_2 compositions and pressures around 1150 psia [7.9 MPa], a crescent-shaped region exists in which three phases (CO_2-rich liquid, oil-rich liquid and vapor) coexist. CO_2 compositions from 0-99 mole% were studied to define the phase envelopes. It was recognized that for CO_2 compositions in excess of 99 mole%, a small two-phase envelop would exist where a vapor phase coexists with the CO_2-rich liquid. Also in this compositional range, there must exist a droplet point curve to mark the boundary between the liquid-liquid region and the single-phase nearly-pure CO_2 fluid. No attempt to locate either of these features was made in this work.

Measurements indicate that the existence of liquid-liquid and liquid-liquid-vapor immiscibility at elevated pressures and high CO_2 compositions is dependent upon the temperature and oil composition. Liquid-liquid-vapor equilibria has not been observed in any of these above 110°F [316.5 K]. The multiple temperature "room" diagram determined for Oil B2 (Figure 3 here and reported earlier)[4] shows the disappearance of three-phase behavior (indicated by the cross hatched regions) with increasing temperature. The region of liquid-liquid immiscibility likewise shrinks in compositional expanse with increased temperature. Quality lines determined in the liquid-liquid region (Figures 4 and 11) indicate the absence of liquid-liquid critical behavior below 3000 psia [21 MPa]. The same was true for all other CO_2-reservoir oil systems studied in this work. Other researchers do report this phenomenon, for example, Gardner, et al.,[5] report a liquid-liquid critical at 1600 psia [11.0 MPa] for the CO_2-Wasson Denver Unit reservoir oil system. Additional measurements made by Orr, et al.,[6] for the same system indicate a lack of liquid-liquid critical behavior at these conditions. Our Oil F system, having a very similar composition to that reported[5] for Wasson Denver Unit oil, exhibited no critical behavior at these conditions as is indicated by the lack of convergence of the quality lines shown in Figure 11. The location of the liquid-liquid critical point may be highly sensitive to the composition of the reservoir oil. The liquid-liquid immiscibility also appears to be related to the C_7+ molecular weight, since oils with higher C_7+ molecular weights appear to have wider and taller liquid-liquid regions on pressure-composition diagrams at the same temperature. The liquid-liquid immiscibility is consistent with the behavior noted for CO_2-hydrocarbon binary systems, which show this behavior at reservoir temperatures for hydrocarbons of greater molecular weight than C_{13}.

As shown in Figures 7 and 8, the loss of light hydrocarbons from the reservoir oil altered the phase diagrams from that determined for the recombined oil from the same reservoir (Figure 5). The pressure range of the three-phase region is decreased dramatically. The phase behavior of these weathered oil systems approaches that exhibited by CO_2-heavy hydrocarbon binary systems, in which three-phase behavior occurs at only a single pressure for a given temperature, as discussed in detail by Orr, et al.[6]

Several other observations are common to the systems studied to date. Phase densities and viscosities were measured at fixed pressures (roughly the anticipated reservoir operating pressures). These properties are plotted in Figures 12-15 as values labeled "First Contact". At low CO_2 compositions, the CO_2-West Texas oil systems show a negative volume change of mixing as shown in Figures 12 and 13; i.e., the mixture densities increase with increasing CO_2 composition. In the liquid-liquid region, the density of the oil-rich phase increases rapidly with increasing CO_2 composition. The density of the CO_2-rich liquid increases with increasing CO_2 composition. Viscosities at low CO_2 compositions show reductions with increasing CO_2 composition as shown in Figures 14 and 15. In the liquid-liquid region the oil-rich phase exhibits high viscosities, while the CO_2-rich phase viscosities are in the vicinity of the pure CO_2 values.

Equilibrium fluid phases were sampled at the anticipated reservoir operating pressures (Table 2) and in the three-phase region (Table 3). It can be seen that the oil-rich liquid phase is capable of dissolving a substantial amount (from 55 mole% to 75 mole% depending upon the conditions) of CO_2. The CO_2-rich liquid phase appears to extract a great deal of the light hydrocarbons from the oil-rich phase. It is also significant that the CO_2-rich liquid phase acquires a significant C_7+ composition which would lead one to believe that, even in an immiscible displacement process, the residual oil saturation predicted by the phase equilibria would be rather low in well swept zones. In the three-phase region, the CO_2-rich liquid and the vapor phase appear very close in composition with the only exception being the C_7+ composition which is higher in the CO_2-rich liquid phase. Thus one could regard the three-phase region as being the narrow pressure range in which the CO_2-rich liquid phase vaporizes with decreasing pressure.

Cycling Studies

Results of these studies are presented in terms of pictorial representations of cell contents (Figures 16-21), equilibrium phase compositions (Tables 4 and 5), phase densities (Figures 12 and 13), and phase viscosities (Figures 14 and 15).
Figures 16-21 display fluid property cell contents graphically at each step in the cycling studies after correction for fluid sampling losses. The oil-rich liquid phase is indicated by the dark cross hatched areas and the CO_2-rich phase is indi-

cated by the lighter lined regions. All volumes are expressed as a percentage of the original fluid volume charged to the equilibrium cell. For example in Figure 17, starting with the original charge of recombined reservoir oil (the left-most bar), sufficient CO_2 was added to give a bulk composition in the cell of 50 mole% CO_2. At this point the cell contained all oil-rich liquid occupying a volume 1.21 times the original oil volume as illustrated by the second bar from the left. Additional CO_2 was added to bring the bulk CO_2 composition to 78 mole%. At this point the cell contained both an oil-rich liquid phase and a CO_2-rich liquid phase. The oil-rich liquid phase occupied a volume 94.1% of the original oil charge and the CO_2-rich liquid occupied a volume 1.097 times that of the original oil charge as illustrated by the center bar. Following sampling, the CO_2-rich liquid phase was removed from the cell and discarded. Additional CO_2 was then added to give a bulk composition of 85 mole% in the cell. Again two phases were present in the cell. The oil-rich liquid occupied a volume 70.0% of the original oil charge and the CO_2-rich liquid occupied a volume 0.886 times that of the original oil charge as shown by the forth bar. Another CO_2 contact was conducted in the same manner and is illustrated by the fifth bar. Thus, this figure gives a schematic representation of the cell contents during the cycling study.

Equilibrium phase compositions obtained during the CO_2 cycling studies are reported in Table 4 together with measured C_7+ molecular weights. As one would expect, CO_2 cycling strips light components from the oil-rich liquid phase increasing the C_7+ molecular weight as shown in Table 4. After three contacts with CO_2, the systems studied here exhibit CO_2 compositions from 66-80 mole% in the oil-rich liquid phases and from 94-99 mole% in the CO_2-rich liquid phases.

Equilibrium phase compositions obtained during the oil cycling studies are reported in Table 5 together with measured C_7+ molecular weights. Oil cycling for the A and B1 systems produced CO_2-rich liquid phases after three oil contacts with virtually the same compositions as the CO_2-rich liquids from the first CO_2 contacts during CO_2 cycling, which indicates that three equilibrium contacts are not sufficient to bank the light hydrocarbons. The five oil cycles completed for the B1 system are not sufficient to reach the point of multiple-contact miscibility, nor do the results indicate whether or not it is possible to achieve miscibility at 2200 psia [15.2 MPa] studied here. Time limitations permitted only one pressure to be studied for each system.

An examination of the phase density and phase viscosity results obtained in the CO_2 and oil cycling studies (Figures 12-15) reveals that these data closely agree with static measurements conducted for the same systems. This is consistent with the above observation that phase compositions attained during these cycling studies are nearly the same as those attained in the static measurements. Oil-rich liquid phase densities in these measurements vary from 0.78 to 0.82 g/cc [780 to 820 kg/m^3] for the original reservoir oils to about 0.94 g/cc [940 kg/m^3] after the third CO_2 contact (roughly 70-80 mole% CO_2 in the oil-rich phase). CO_2-rich liquid phase densities are scattered from 0.73 to 0.78 g/cc [730-780 kg/m^3] with a slight upward trend with higher CO_2 compositions. For comparison purposes, densities of pure CO_2 from the literature[7] were also included in Figures 12 and 13. Viscosities of the recombined reservoir oils range from 1.2 to 2.6 cp [0.0012 to 0.0026 Pa-s]. Viscosities of the oil-rich liquids decrease with increasing CO_2 composition up to the start of liquid-liquid immiscibility. At this point the oil-rich viscosities are about half as large as those of the recombined oils. In the liquid-liquid region the oil-rich phase viscosities increase sharply with increasing CO_2 composition. CO_2-rich liquid phase viscosities are scattered around 0.1 cp [0.0001 Pa-s] and show a slight decrease with increasing CO_2 composition. For comparison, viscosities of pure CO_2 from the literature[8] were included in Figures 14 and 15. As discussed earlier, viscosities measured for the CO_2-rich phase are highly uncertain (±50%) due to limitations of the viscometer available for this work.

More CO_2 or oil cycles could have been run in these studies but experimental uncertainties are cumulative, and for that reason, it is doubtful whether measurements from a large number of cycles in the fluid property cell could be compared to slim tube displacements or core flood results, which involve a large number of equilibrium contacts. Cycling studies in this work show qualitative trends and will be useful in testing predictive tools being developed for these systems.

CONCLUSIONS

1. Differences noted among these West Texas-CO_2 systems are related primarily to reservoir temperatures and to a lesser extent reservoir oil compositions. No liquid-liquid-vapor regions have been observed above $110^{\circ}F$ [316.5 K].

2. No liquid-liquid critical point was observed for any of the CO_2-West Texas systems studied to date.

3. The CO_2-rich liquid phase, which exists at high CO_2 compositions, pressures above 1300 psia [9 MPa], and temperatures around $110^{\circ}F$ [316.5 K] and below, is capable of extracting a significant portion of all but the heaviest hydrocarbon components present in the original reservoir oil.

4. Multiple contact measurements simulating phase behavior of residual oil remaining after being contacted with large quantities of CO_2 confirm the residual oil-rich liquid phase will have a very high viscosity and a composition of approximately 80 mole% CO_2 with the remainder being very heavy hydrocarbons and will occupy only a small fraction of the original oil volume.

5. Multiple contact measurements simulating phase behavior at the flood front reveal no appreciable banking of light hydrocarbons in the CO_2-rich liquid phase as has been observed in corefloods. Most likely, the finite number of equilibrium contacts that can be attained in a fluid property cell is not sufficient to reveal this anticipated multiple contact effect.

REFERENCES

1. Jacoby, Robert H. and Yarborough, Lyman: "PVT Measurements on Petroleum Reservoir Fluids and Their Uses," Industrial Engineering Chemistry, 59, 48-62, October 1967.

2. Yarborough, Lyman and Vogel, John L.: "A New System for Obtaining Vapor and Liquid Analyses to Facilitate the Study of Multicomponent Mixtures at Elevated Pressures," Chemical Engineering Progress Symposium Series, 63(81), 1-9, 1967.

3. Yarborough, Lyman: "Vapor-Liquid Equilibrium Data for Multicomponent Mixtures Containing Hydrocarbon and Nonhydrocarbon Components," Journal of Chemical and Engineering Data, 17, 129-133, April 1972.

4. Turek, E. A., Metcalfe, R. S., Yarborough L. and Robinson, R. L., Jr.: "Phase Equilibria in Carbon Dioxide + Multicomponent Hydrocarbon Systems: Experimental Data and an Improved Prediction Technique," Society of Petroleum Engineers Journal, in press.

5. Gardner, J. W., Orr, F. M. and Patel, P. D.: "The Effect of Phase Behavior on CO_2 Flood Displacement Efficiency," SPE Paper 8367, 54th Annual Technical Conference and Exhibition of the Society of Petroleum Engineers of AIME, Las Vegas, September 23, 1979.

6. Orr, F. M. and Jensen, C. M.: "Interpretation of Pressure-Composition Phase Diagrams for CO_2-Crude Oil Systems," SPE Paper 11125, 57th Annual Technical Conference and Exhibition of the Society of Petroleum Engineers of AIME, New Orleans, September 26, 1982.

7. Angus, S., Armstrong, B. and de Reuck, K. M.: International Thermodynamic Tables of the Fluid State of Carbon Dioxide, Pergamon Press, New York, 1976, pp. 84-177.

8. Stephan, K. and Lucas, K.: Viscosity of Dense Fluids, Plenum Press, New York, 1979, pp. 75-79.

Table 1
Oil Compositional Analyses

Component	Recombined Oil A	Recombined Oil B1	Recombined Oil B2	Recombined Oil C1	Oil C1 Weathered 24 Hours at 75°F	Oil C1 Weathered 24 Hours at 104°F	Recombined Oil C2	Recombined Oil D	Recombined Oil E	Recombined Oil F
Total Fluid Compositions (Mole %)										
N_2	1.27	0.52	0.47	--	0.00	0.00	--	--	--	0.58
C_1	16.08	15.43	12.65	19.80	0.00	0.00	18.34	12.62	31.49	15.57
CO_2	4.17	0.56	0.42	0.00	0.00	0.00	0.01	0.00	0.29	4.58
C_2	8.43	7.26	6.65	6.38	0.00	0.00	7.78	3.80	11.18	13.25
H_2S	1.69	--	--	--	--	--	--	3.80	--	0.32
C_3	7.48	6.14	6.91	6.64	0.00	0.00	7.91	4.80	13.49	9.53
iC_4	1.63	0.49	1.57	0.42	0.00	0.00	0.65	1.09	4.20	1.72
nC_4	3.85	4.10	4.61	4.32	0.06	0.00	4.74	2.92	8.31	4.36
iC_5	1.74	1.36	2.40	0.98	1.07	0.00	1.65	1.54	0.39	0.84
nC_5	2.11	2.69	2.84	1.46	1.50	0.02	1.78	1.86	3.19	3.42
C_6s	4.30	3.61	2.92	2.49	2.01	0.06	3.82	2.44	1.07	3.72
C_7+	47.25	57.84	58.56	57.51	95.36	99.92	53.32	68.93	26.39	42.11
	100.00	100.00	100.00	100.00	100.00	100.00	100.00	100.00	100.00	100.00
C_7+ Boiling Point Breakdowns (Mole %) and C_7+ Properties										
C_7s	12.34	12.13	12.60	11.27	2.52	0.20	10.55	9.89	8.46	10.99
C_8s	10.03	12.39	11.08	13.21	7.02	1.07	12.07	9.53	10.61	11.77
C_9s	8.05	10.76	10.15	11.63	11.96	5.53	14.19	9.91	11.93	7.44
C_{10}s	6.73	6.75	9.88	7.70	10.96	7.14	5.79	7.94	8.83	6.29
C_{11}s	6.18	5.14	4.47	6.21	8.62	7.93	4.48	5.30	7.55	5.09
C_{12}s	4.93	4.34	4.19	5.39	6.85	6.95	4.07	2.67	6.88	4.38
C_{13}s	4.53	4.09	3.42	4.80	5.73	6.78	3.97	4.71	5.57	4.17
C_{14}s	4.08	3.87	3.70	4.63	3.99	5.27	4.24	4.32	5.16	4.19
C_{15}s	4.16	3.74	3.51	3.74	3.41	5.69	3.96	3.15	3.78	4.15
C_{16}s	3.74	3.09	3.14	3.30	3.53	4.08	3.46	3.96	3.34	3.69
C_{17}s	3.39	3.23	3.36	3.30	3.48	3.95	3.83	4.16	3.33	3.51
C_{18}s	2.97	3.10	3.22	2.72	3.18	4.15	2.63	2.92	2.78	3.19
C_{19}s	2.60	2.47	2.45	2.27	1.95	4.37	2.58	2.55	2.48	2.85
C_{20}s	2.17	2.18	2.27	2.12	1.86	3.04	2.87	2.58	1.98	2.41
C_{21}s	1.96	2.23	1.99	1.79	2.12	2.77	1.99	2.30	1.84	2.26
C_{22}s	1.97	1.98	2.02	1.56	1.93	2.12	1.88	2.05	1.35	0.92
C_{23}s	1.18	1.75	1.12	1.21	1.92	2.00	1.50	2.04	1.47	1.87
C_{24}s	0.67	1.55	1.41	1.14	1.26	1.60	1.38	1.29	1.12	1.62
C_{25}s	1.20	1.56	1.16	0.99	0.73	1.62	0.88	1.45	1.04	1.13
C_{26}s	1.15	1.38	1.06	0.90	1.19	1.60	1.15	0.95	0.95	1.32
C_{27}s	1.27	1.24	1.00	0.81	1.21	1.82	1.02	0.99	0.82	1.31
C_{28}s	0.48	1.10	0.96	0.75	1.12	1.74	0.97	1.19	0.79	0.90
C_{29}s	0.98	0.97	0.86	0.87	0.73	1.57	0.89	1.02	0.69	1.21
C_{30}s	0.92	0.81	0.81	0.77	1.19	1.36	0.82	0.90	0.61	1.08
C_{31}s	1.02	0.73	0.89	0.51	0.73	0.85	0.74	1.14	0.80	0.84
C_{32}s	0.59	0.65	0.62	0.37	0.61	0.92	0.82	0.86	0.42	0.66
C_{33}s	0.94	0.58	0.62	0.39	0.69	1.10	0.60	0.62	0.61	0.86
C_{34}s	0.67	0.52	0.55	0.72	0.73	1.10	0.54	0.74	0.61	1.20
C_{35}s	0.75	0.46	0.66	0.39	0.58	1.33	0.61	0.64	0.28	0.95
C_{36}s	0.93	0.40	0.52	0.60	0.67	0.83	0.81	1.23	0.22	0.74
C_{37}s	0.56	0.36	0.50	0.25	0.78	0.99	0.59	0.70	0.17	0.85
C_{38}s	0.45	0.32	0.46	0.23	0.44	0.66	0.32	1.07	0.25	0.74
C_{39}s	0.41	0.29	0.41	0.18	0.44	0.59	0.28	0.30	0.11	0.69
C_{40}+	6.00	3.84	4.94	3.28	5.87	7.28	3.52	4.93	3.17	4.73
	100.00	100.00	100.00	100.00	100.00	100.00	100.00	100.00	100.00	100.00
C_7+ Mol. Wt.	253	226	233	215	251	290	230	247	226	243
C_7+ Sp.Grav.	0.8896	0.8822	0.8880	0.8505	--	--	0.8763	0.8917	0.8593	0.8839

Table 2
Equilibrium Compositions in the Two-Phase Region

	Phase Compositions (Mole%)									
	Oil B2 75 Mole% CO_2 Bulk 106°F and 2200 psia		Oil B2 85 Mole% CO_2 Bulk 106°F and 2200 psia		Oil B2 95 Mole% CO_2 Bulk 106°F and 2200 psia		Oil C2 75 Mole% CO_2 Bulk 94°F and 1700 psia		Oil C2 80 Mole% CO_2 Bulk 94°F and 1700 psia	
Component	Oil-Rich Liquid	CO_2-Rich Liquid	Oil-Rich Liquid	CO_2-Rich Liquid	Oil-Rich Liquid	CO_2-Rich Liquid	Oil-Rich Liquid	CO_2-Rich Liquid	Oil-Rich Liquid	CO_2-Rich Liquid
N_2	0.00	0.23	0.00	0.10		0.04	0.12	0.08	0.19	0.06
C_1	2.96	3.80	1.58	2.17		0.64	4.77	5.42	3.40	3.87
CO_2	66.71	86.07	67.69	92.01	(b)	97.14	66.86	81.83	67.60	85.80
C_2	1.99	1.95	1.35	1.10		0.30	2.55	2.24	2.14	1.60
H_2S (a)	--	--	--	--		--	--	--	--	--
C_3	1.89	1.94	1.24	1.17		0.37	2.52	2.00	2.21	1.55
iC_4	0.42	0.48	0.14	0.28		0.02	0.25	0.18	0.21	0.19
nC_4	1.20	1.21	0.82	0.74		0.24	1.73	1.18	1.61	0.94
iC_5	0.46	0.66	0.30	0.41		0.13	0.75	0.45	0.98	0.37
nC_5	0.53	0.82	0.35	0.52		0.19	1.01	0.58	1.00	0.45
C_6s	0.46	0.55	0.46	0.28		0.19	1.64	0.92	2.78	0.78
C_7+	23.38	2.29	26.07	1.22		0.74	17.80	5.12	17.88	4.39
	100.00	100.00	100.00	100.00		100.00	100.00	100.00	100.00	100.00

	Oil C2 90 Mole% CO_2 Bulk 94°F and 1700 psia		Oil D 71 Mole% CO_2 Bulk 105°F and 2000 psia		Oil D 80 Mole% CO_2 Bulk 105°F and 2000 psia		Oil D 85 Mole% CO_2 Bulk 105°F and 2000 psia		Oil D 95 Mole% CO_2 Bulk 105°F and 2000 psia	
Component	Oil-Rich Liquid	CO_2-Rich Liquid	Oil-Rich Liquid	CO_2-Rich Liquid	Oil-Rich Liquid	CO_2-Rich Liquid	Oil-Rich Liquid	CO_2-Rich Liquid	Oil-Rich Liquid	CO_2-Rich Liquid
N_2	0.04	0.03	0.00	0.07		0.07	0.00	0.02	0.00	
C_1	1.66	1.64	4.17	5.32		3.20	1.80	2.40	0.53	
CO_2	72.97	93.88	65.50	86.54	(b)	90.91	65.91	93.89	66.22	(b)
C_2	1.28	0.83	1.24	1.18		0.75	0.68	0.56	0.00	
H_2S (a)	--	--	--	--		--	--	--	--	
C_3	1.17	0.62	1.33	1.52		1.08	0.73	0.75	0.00	
iC_4	0.13	0.06	0.32	0.42		0.29	0.27	0.21	0.00	
nC_4	1.91	0.38	1.20	1.33		0.96	0.81	0.64	0.38	
iC_5	0.39	0.16	0.41	0.66		0.45	0.00	0.32	0.00	
nC_5	0.53	0.19	0.35	0.76		0.53	0.00	0.38	0.00	
C_6s	1.05	0.33	0.74	0.52		0.36	0.50	0.25	0.34	
C_7+	18.87	1.88	24.74	1.68		1.40	29.30	0.58	32.53	
	100.00	100.00	100.00	100.00		100.00	100.00	100.00	100.00	

	Oil E 75 Mole% CO_2 Bulk 120°F and 1750 psia		Oil E 85 Mole% CO_2 Bulk 120°F and 1750 psia		Oil E 95 Mole% CO_2 Bulk 120°F and 1750 psia	
Component	Liquid	Vapor	Liquid	Vapor	Liquid	Vapor
N_2	0.00	0.06		0.03	0.00	0.04
C_1	4.89	7.50		2.25	0.83	1.52
CO_2	58.53	81.01	(b)	94.12	61.48	96.07
C_2	2.68	2.82		0.76	0.60	0.42
H_2S (a)	--	--		--	--	--
C_3	3.49	3.41		1.05	0.75	0.70
iC_4	0.00	0.02		0.00	0.00	0.00
nC_4	3.38	3.15		1.01	0.83	0.67
iC_5	0.00	0.12		0.04	0.00	0.03
nC_5	0.75	0.89		0.32	0.22	0.21
C_6s	0.26	0.21		0.08	0.22	0.05
C_7+	26.02	0.81		0.34	35.07	0.29
	100.00	100.00		100.00	100.00	100.00

Notes:

(a) - Analytical procedures and equipment were incapable of detecting small concentrations of H_2S.

(b) - Inconsistent analyses were obtained for these phases due to sampling or analytic errors.

Table 3
Equilibrium Compositions in the Three-Phase Region

	Phase Compositions (Mole %)														
	Oil B2 70 Mole% CO_2 Bulk 106°F + 1306 psia			Oil B2 80 Mole% CO_2 Bulk 106°F + 1250 psia			Oil B2 90 Mole% CO_2 Bulk 106°F + 1245 psia			Oil B2 95 Mole% CO_2 Bulk 106°F + 1249 psia			Oil C2 75 Mole% CO_2 Bulk 94°F + 1135 psia		
Component	Oil-Rich Liquid	CO_2-Rich Liquid	Vapor	Oil-Rich Liquid	CO_2-Rich Liquid	Vapor	Oil-Rich Liquid	CO_2-Rich Liquid	Vapor	Oil-Rich Liquid	CO_2-Rich Liquid	Vapor	Oil-Rich Liquid	CO_2-Rich Liquid	Vapor
N_2	0.00	0.00	0.00	0.02	0.00	0.00	0.02	0.00	0.09	0.00	0.00	0.00	0.16	0.03	0.11
C_1	3.36	4.83	6.64	2.00	2.58	3.79	0.43	1.28	1.81	0.61	0.69	0.61	3.35	4.07	8.55
CO_2	63.75	86.33	87.60	59.66	89.11	92.68	53.10	94.24	95.57	64.02	95.62	97.25	66.28	83.64	87.30
C_2	2.29	1.73	0.97	1.59	0.90	1.09	0.78	0.69	0.71	0.53	0.33	0.32	2.34	1.87	1.94
H_2S (a)	--	--	--	--	--	--	--	--	--	--	--	--	--	--	--
C_3	2.31	1.57	1.08	1.69	1.09	0.85	0.86	0.69	0.57	0.54	0.33	0.31	2.43	1.93	0.73
iC_4	0.52	0.33	0.25	0.38	0.29	0.15	0.20	0.15	0.11	0.12	0.07	0.07	0.25	0.20	0.09
nC_4	1.43	0.86	0.62	1.17	0.77	0.39	1.66	0.42	0.28	0.45	0.19	0.19	1.78	1.24	0.49
iC_5	0.55	0.38	0.28	0.54	0.39	0.15	0.32	0.20	0.11	0.27	0.09	0.09	0.75	0.49	0.14
nC_5	0.58	0.45	0.32	0.65	0.49	0.17	0.40	0.24	0.14	0.31	0.11	0.12	0.98	0.59	0.15
C_6s	0.64	0.55	0.39	0.61	0.65	0.18	0.34	0.32	0.15	0.07	0.07	0.07	1.80	1.01	0.18
C_7+	24.57	2.97	1.85	31.69	3.73	0.55	41.89	1.77	0.46	33.08	2.50	0.97	19.88	4.93	0.32
	100.00	100.00	100.00	100.00	100.00	100.00	100.00	100.00	100.00	100.00	100.00	100.00	100.00	100.00	100.00

	Oil C2 80 Mole% CO_2 Bulk 94°F + 1132 psia			Oil C2 90 Mole% CO_2 Bulk 94°F + 1084 psia			Oil D 71 Mole% CO_2 Bulk 105°F + 1300 psia			Oil D 80 Mole% CO_2 Bulk 105°F + 1252 psia			Oil D 85 Mole% CO_2 Bulk 105°F + 1223 psia		
Component	Oil-Rich Liquid	CO_2-Rich Liquid	Vapor	Oil-Rich Liquid	CO_2-Rich Liquid	Vapor	Oil-Rich Liquid	CO_2-Rich Liquid	Vapor	Oil-Rich Liquid	CO_2-Rich Liquid	Vapor	Oil-Rich Liquid	CO_2-Rich Liquid	Vapor
N_2	0.13	0.05	0.07	0.21	0.03	0.09	0.00	0.07	0.11	0.00	0.05	0.07	0.00		0.07
C_1	3.12	4.28	7.18	0.99	1.27	3.33	2.15	5.37	7.59	1.93	3.27	4.72	0.00		0.75
CO_2	64.94	84.31	88.58	68.08	93.29	94.58	52.03	88.64	88.13	64.38	89.77	92.48	53.17	(b)	98.32
C_2	2.26	2.13	1.69	0.84	0.89	0.89	0.00	1.21	1.18	0.79	0.71	0.75	0.00		0.16
H_2S (a)	--	--	--	--	--	--	--	--	--	--	--	--	--		--
C_3	2.60	1.95	1.08	1.17	0.74	0.50	0.00	1.31	1.13	0.96	0.91	0.75	0.00		0.19
iC_4	0.27	0.18	0.08	0.13	0.08	0.03	0.00	0.35	0.25	0.00	0.24	0.17	0.00		0.05
nC_4	1.87	1.17	0.47	0.96	0.50	0.21	0.29	1.05	0.74	0.93	0.73	0.47	0.30		0.16
iC_5	0.81	0.44	0.14	0.46	0.21	0.06	0.00	0.46	0.26	0.23	0.33	0.18	0.00		0.07
nC_5	1.05	0.54	0.15	0.91	0.25	0.07	0.00	0.52	0.29	0.00	0.39	0.19	0.00		0.08
C_6s	1.88	0.87	0.19	1.27	0.44	0.08	0.30	0.31	0.14	0.37	0.56	0.10	0.31		0.05
C_7+	21.07	4.08	0.37	24.98	2.30	0.16	45.23	0.71	0.18	30.41	3.04	0.12	46.22		0.10
	100.00	100.00	100.00	100.00	100.00	100.00	100.00	100.00	100.00	100.00	100.00	100.00	100.00		100.00

Notes:
(a) - Analytical procedures and equipment were incapable of detecting small concentrations of H_2S.
(b) - Inconsistent analyses were obtained for this phase due to sampling or analytic errors.

Table 4
Equilibrium Compositions in the CO_2 Cycling Studies

Phase Compositions (Mole%)

	Oil A at 2015 psia and 105°F						Oil B1 at 2015 psia and 106°F					
	First Contact		Second Contact		Third Contact		First Contact		Second Contact		Third Contact	
	75 Mole% CO_2 Bulk		85 Mole% CO_2 Bulk		95 Mole% CO_2 Bulk		78 Mole% CO_2 Bulk		85 Mole% CO_2 Bulk		95 Mole% CO_2 Bulk	
Component	Oil-Rich Liquid	CO_2-Rich Liquid	Oil-Rich Liquid	CO_2-Rich Liquid	Oil-Rich Liquid	CO_2-Rich Liquid	Oil-Rich Liquid	CO_2-Rich Liquid	Oil-Rich Liquid	CO_2-Rich Liquid	Oil-Rich Liquid	CO_2-Rich Liquid
N_2	0.21	0.37	0.05	0.15	0.08	0.02	0.07	0.13	0.02	0.05	0.00	0.01
C_1	3.47	4.30	1.05	2.24	0.19	0.15	2.88	3.62	0.96	1.25	0.10	0.15
CO_2	65.14	82.30	69.95	86.53	71.05	97.86	65.12	85.11	65.62	92.43	65.72	97.65
C_2	2.29	2.11	0.93	1.38	0.15	0.13	1.74	1.59	0.76	0.67	0.13	0.11
H_2S (a)	--	--	--	--	--	--	--	--	--	--	--	--
C_3	2.25	1.84	1.03	1.30	0.20	0.14	1.61	1.26	0.77	0.56	0.16	0.10
iC_4	0.28	0.22	0.14	0.17	0.03	0.02	0.12	0.10	0.07	0.05	0.01	0.01
nC_4	1.54	1.05	0.82	0.84	0.20	0.11	1.27	0.81	0.76	0.44	0.20	0.10
iC_5	0.54	0.35	0.30	0.28	0.08	0.04	0.42	0.26	0.26	0.14	0.07	0.03
nC_5	1.18	0.72	0.72	0.62	0.24	0.11	0.89	0.56	0.58	0.28	0.19	0.07
C_6s	1.19	0.67	0.79	0.58	0.27	0.10	1.21	0.72	0.86	0.36	0.31	0.10
C_7+	21.91	6.07	24.22	5.91	27.51	1.32	24.67	5.84	29.34	3.77	33.11	1.67
	100.00	100.00	100.00	100.00	100.00	100.00	100.00	100.00	100.00	100.00	100.00	100.00
C_7+ Mol. Wt.	286	167	318	169	342	183	265	154	301	162	368	168

	Oil C1 at 1615 psia and 94°F						Oil F at 2015 psia and 105°F					
	First Contact		Second Contact		Third Contact		First Contact		Second Contact		Third Contact	
	80 Mole% CO_2 Bulk		92 Mole% CO_2 Bulk		95 Mole% CO_2 Bulk		65 Mole% CO_2 Bulk		75 Mole% CO_2 Bulk		89 Mole% CO_2 Bulk	
Component	Oil-Rich Liquid	CO_2-Rich Liquid	Oil-Rich Liquid	CO_2-Rich Liquid	Oil-Rich Liquid	CO_2-Rich Liquid	Oil-Rich Liquid	CO_2-Rich Liquid	Oil-Rich Liquid	CO_2-Rich Liquid	Oil-Rich Liquid	CO_2-Rich Liquid
N_2	0.02	0.04	0.01	0.02	0.01	0.01	0.19	0.27	0.07	0.16	0.20	0.00
C_1	4.77	5.39	0.84	0.84	0.11	0.06	6.21	7.10	3.16	4.15	0.54	0.79
CO_2	69.85	83.05	77.47	95.58	80.42	99.07	59.21	68.02	63.21	80.00	68.72	94.23
C_2	2.29	1.96	0.72	0.53	0.25	0.10	5.44	5.42	3.40	3.35	0.96	0.80
H_2S (a)	--	--	--	--	--	--	--	--	--	--	--	--
C_3	2.41	1.90	0.72	0.43	0.16	0.05	4.12	3.84	2.76	2.40	0.91	0.63
iC_4	0.14	0.11	0.05	0.03	0.01	0.00	0.76	0.70	0.53	0.45	0.20	0.12
nC_4	1.99	1.35	0.71	0.34	0.19	0.05	2.64	2.28	2.02	1.53	0.85	0.43
iC_5	0.54	0.35	0.00	0.09	0.07	0.02	0.59	0.50	0.46	0.33	0.20	0.10
nC_5	1.20	0.73	0.22	0.20	0.17	0.05	0.79	0.65	0.64	0.43	0.35	0.13
C_6s	1.67	0.95	0.45	0.28	0.30	0.06	1.32	1.03	1.13	0.69	0.61	0.22
C_7+	15.12	4.17	18.81	1.66	18.31	0.53	18.73	10.19	22.62	6.51	26.46	2.55
	100.00	100.00	100.00	100.00	100.00	100.00	100.00	100.00	100.00	100.00	100.00	100.00
C_7+ Mol. Wt.	224	154	299	159	332	165	211	191	230	178	258	177

Note:
(a) - Analytical procedures and equipment were incapable of detecting small concentrations of H_2S.

Table 5
Equilibrium Compositions in the Oil Cycling Studies

Phase Compositions (Mole%)

Oil A at 2015 psia and 105°F

Component	First Contact		Second Contact		Third Contact	
	92 Mole% CO_2 Bulk		84 Mole% CO_2 Bulk		78 Mole% CO_2 Bulk	
	Oil-Rich Liquid	CO_2-Rich Liquid	Oil-Rich Liquid	CO_2-Rich Liquid	Oil-Rich Liquid	CO_2-Rich Liquid
N_2	0.00	0.13	0.07	0.25	0.10	0.48
C_1	0.63	1.48	1.32	3.12	2.09	4.93
CO_2	64.43	92.59	64.08	85.49	62.67	81.03
C_2	0.56	0.78	1.05	1.61	1.54	2.41
H_2S (a)	--	--	--	--	--	--
C_3	0.60	0.70	1.15	1.44	1.66	2.33
iC_4	0.08	0.09	0.15	0.18	0.22	0.28
nC_4	0.49	0.45	0.86	0.90	1.24	1.04
iC_5	0.18	0.15	0.31	0.30	0.46	0.29
nC_5	0.42	0.31	0.69	0.60	0.96	0.57
C_6s	0.47	0.30	0.79	0.59	1.06	0.58
C_7+	32.14	3.02	29.53	5.52	28.00	6.06
	100.00	100.00	100.00	100.00	100.00	100.00
C_7+ Mol. Wt.	335	164	281	160	252	161

Oil B1 at 2015 psia and 106°F

Component	First Contact		Second Contact		Third Contact		Fourth Contact		Fifth Contact	
	95 Mole% CO_2 Bulk		90 Mole% CO_2 Bulk		86 Mole% CO_2 Bulk		81 Mole% CO_2 Bulk		76 Mole% CO_2 Bulk	
	Oil-Rich Liquid	CO_2-Rich Liquid	Oil-Rich Liquid	CO_2-Rich Liquid	Oil-Rich Liquid	CO_2-Rich Liquid	Oil-Rich Liquid	CO_2-Rich Liquid	Oil-Rich Liquid	CO_2-Rich Liquid
N_2	0.02	0.03	0.02	0.09	0.03	0.13	0.04	0.17	0.09	0.15
C_1	0.60	0.76	1.24	1.73	1.90	2.30	2.85	3.23	3.65	4.34
CO_2	68.31	95.33	67.91	91.54	67.54	87.67	66.62	83.63	65.45	79.70
C_2	0.45	0.38	0.91	0.89	1.28	1.13	1.67	1.57	2.12	2.07
H_2S (a)	--	--	--	--	--	--	--	--	--	--
C_3	0.44	0.31	0.88	0.77	1.22	0.93	1.41	1.29	1.91	1.70
iC_4	0.03	0.03	0.08	0.05	0.11	0.09	0.10	0.11	0.16	0.13
nC_4	0.43	0.24	0.79	0.45	1.04	0.71	1.06	0.94	1.44	1.14
iC_5	0.15	0.08	0.27	0.14	0.35	0.23	0.35	0.29	0.47	0.36
nC_5	0.33	0.15	0.58	0.28	0.75	0.45	0.78	0.59	0.97	0.71
C_6s	0.50	0.20	0.84	0.35	1.04	0.60	1.08	0.75	1.30	0.90
C_7+	28.74	2.49	26.48	3.71	24.74	5.76	24.04	7.43	22.44	8.80
	100.00	100.00	100.00	100.00	100.00	100.00	100.00	100.00	100.00	100.00
C_7+ Mol. Wt.	350	169	289	160	255	161	238	159	233	158

Note:
(a) - Analytical procedures and equipment were incapable of detecting small concentrations of H_2S.

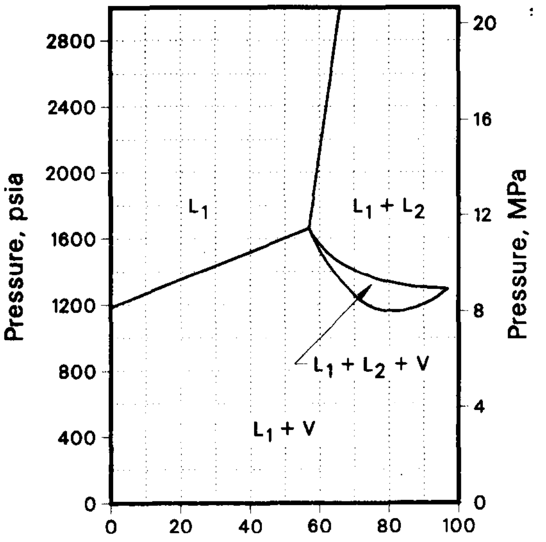

Figure 1 - Oil A - CO_2 phase diagram at 105°F (313.7 K)

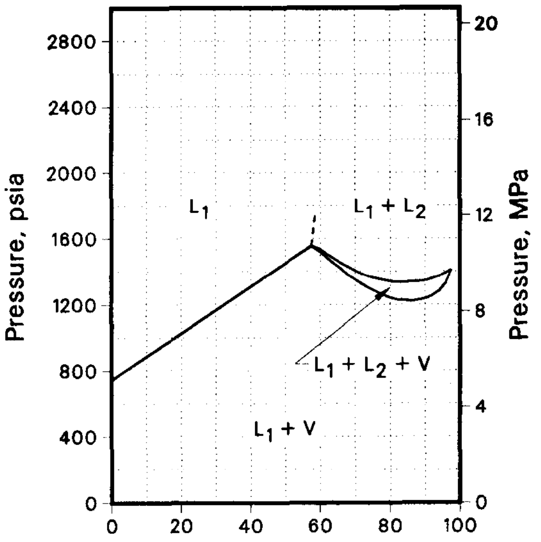

Figure 2 - Oil B1 - CO_2 phase diagram at 106°F (314.3 K)

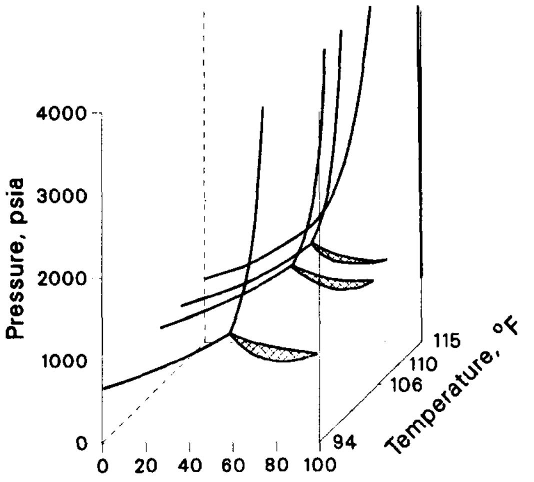

Figure 3 - Oil B2 - CO_2 room diagram

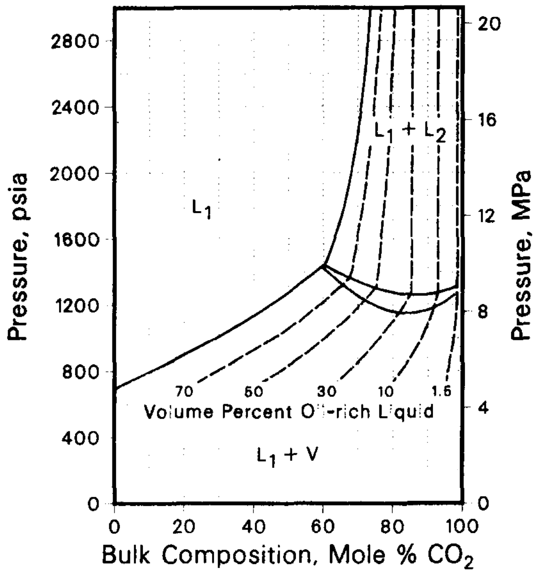

Figure 4 - Oil B2 - CO_2 phase diagram at 106°F (314.3 K)

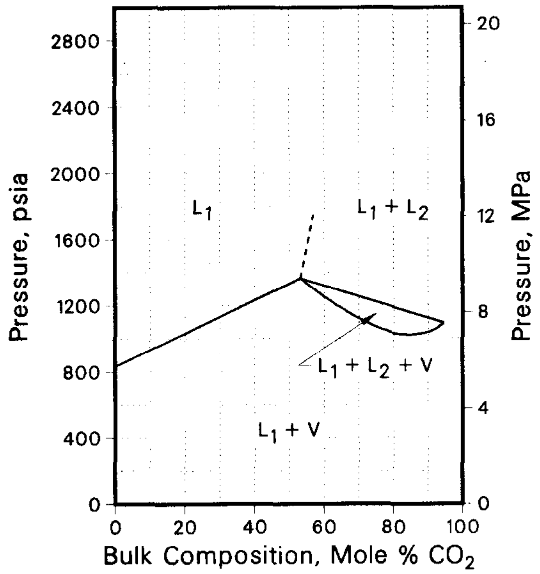

Figure 5 - Oil C2 - CO_2 phase diagram at 94°F (307.6 K)

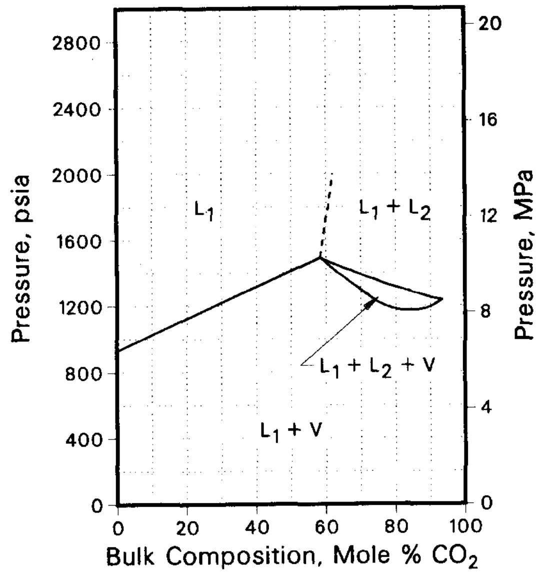

Figure 6 - Oil C2 - CO_2 phase diagram at 105°F (313.7 K)

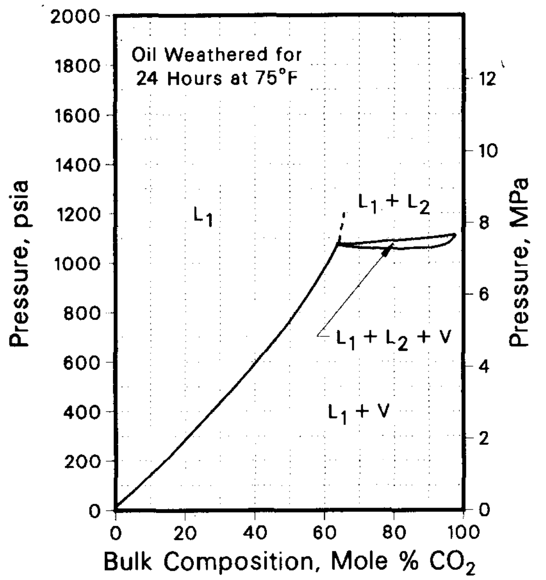

Figure 7 - Weathered oil Cl - CO_2 phase diagram at 94°F (307.6 K)

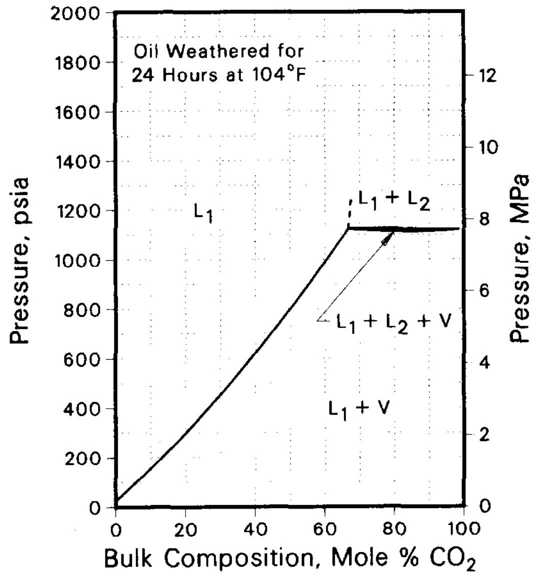

Figure 8 - Weathered oil Cl - CO_2 phase diagram at 94°F (307.6 K)

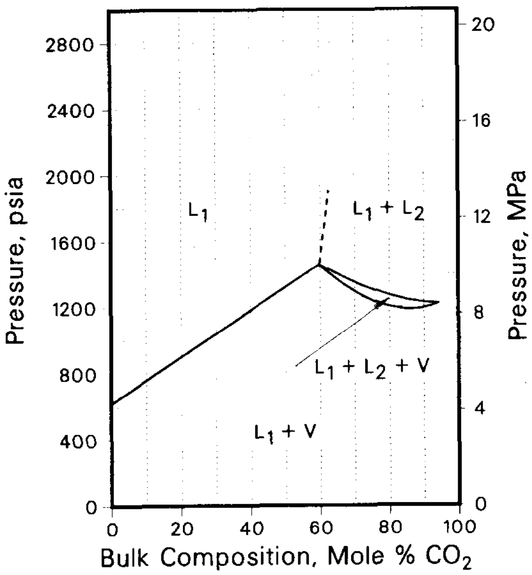

Figure 9 - Oil D - CO_2 phase diagram at 105°F (313.7 K)

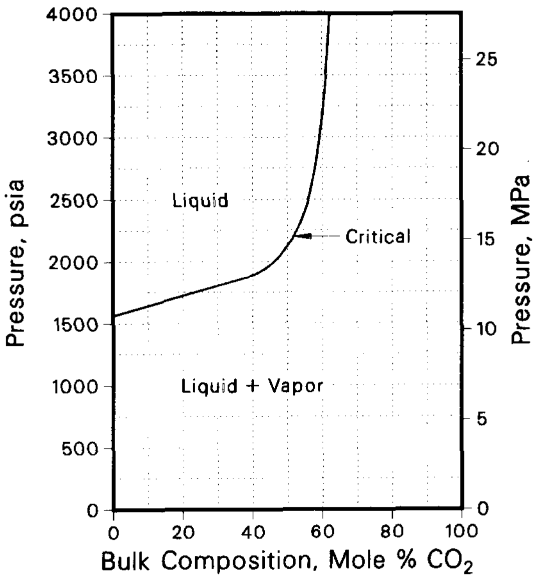

Figure 10 - Oil E - CO_2 phase diagram at 120°F (322.0 K)

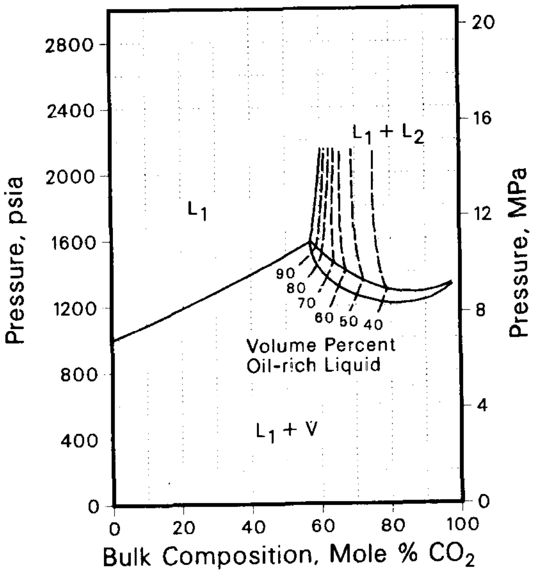

Figure 11 - Oil F - CO_2 phase diagram at 105°F (313.7 K)

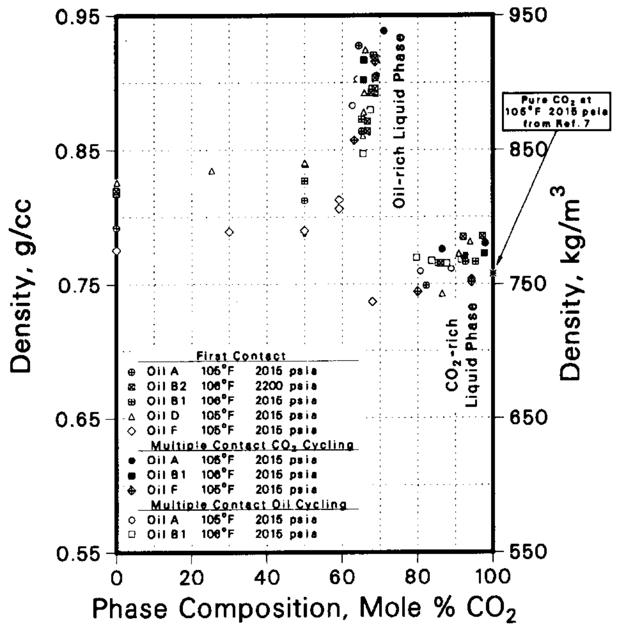

Figure 12 - Phase densities of the San Andres Reservoir oil - CO_2 systems

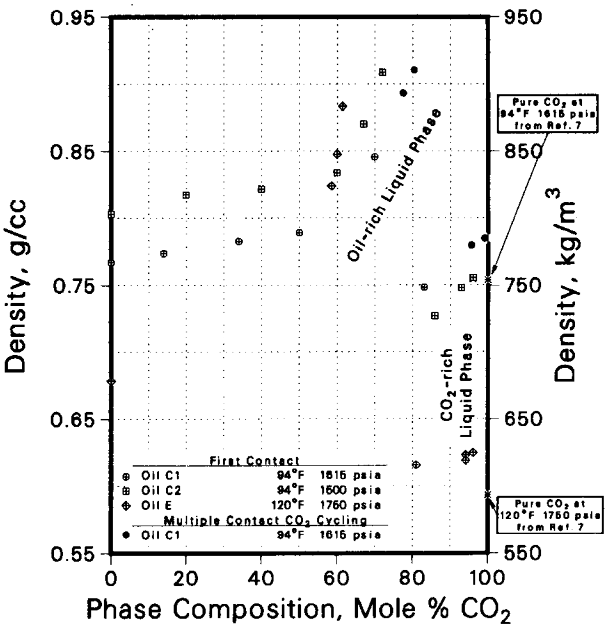

Figure 13 - Phase densities for CO_2 mixtures with Grayburg and Devonian Chert reservoir oils

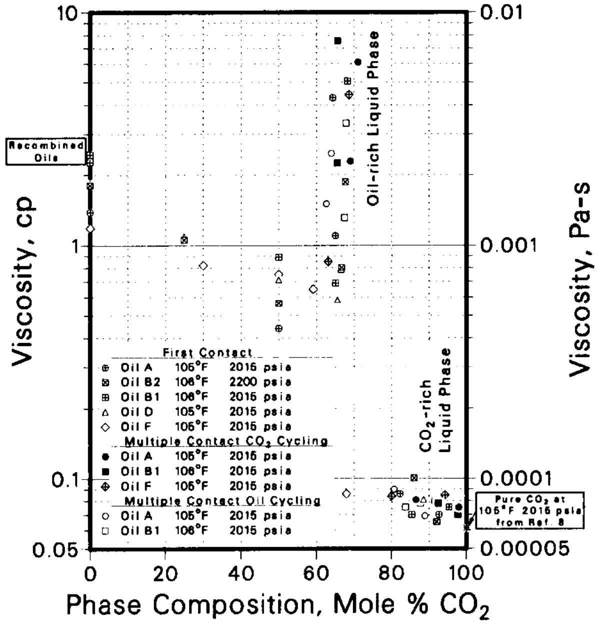

Figure 14 - Phase viscosities of the San Andres Reservoir oil - CO_2 systems

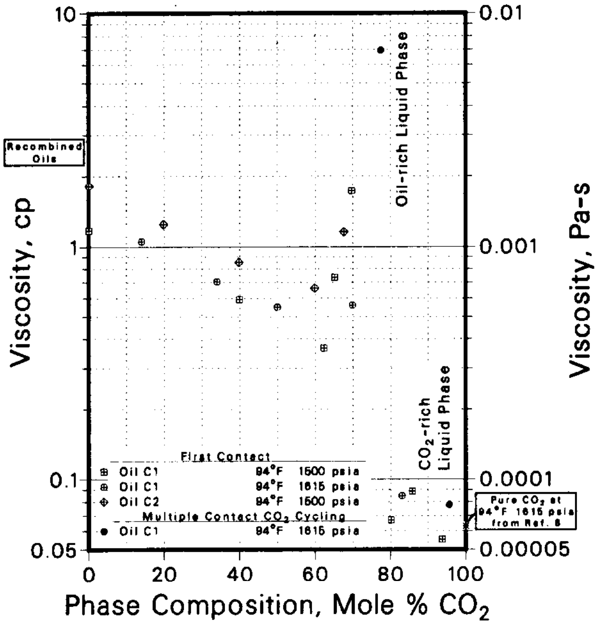

Figure 15 - Phase viscosities of the Grayburg Reservoir oil - CO_2 systems

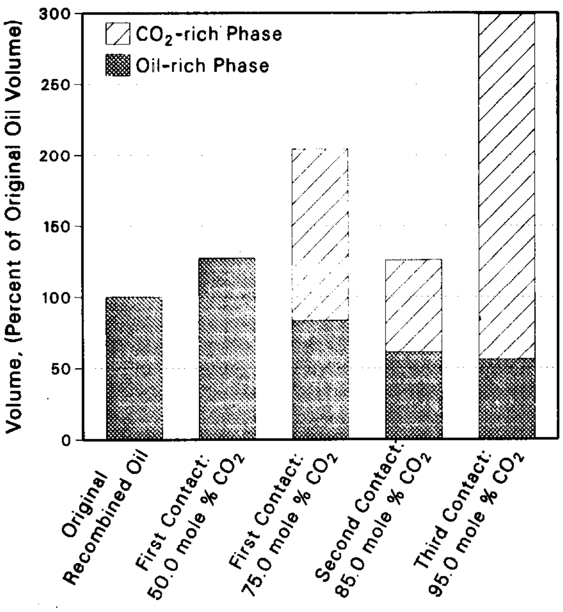

Figure 16 - Phase distributions in Oil A - CO_2 system CO_2 cycling study at 105°F and 2015 psia (313.7 K and 13.89 MPa)

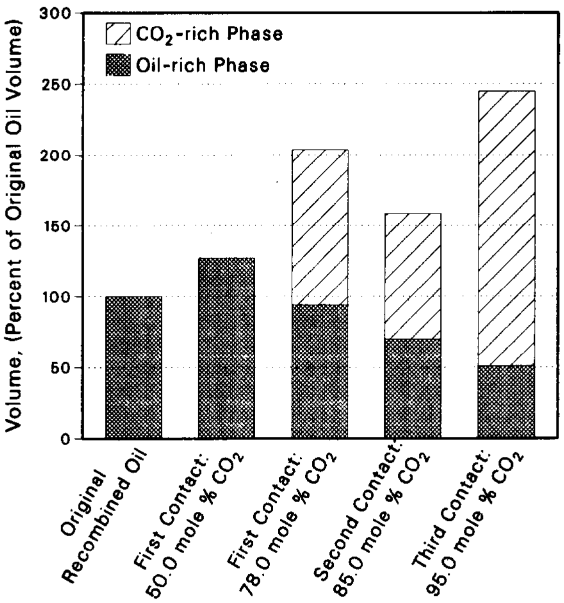

Figure 17 - Phase distributions in Oil B1 - CO_2 system CO_2 cycling study at 106°F and 2015 psia (314.3 K and 13.89 MPa)

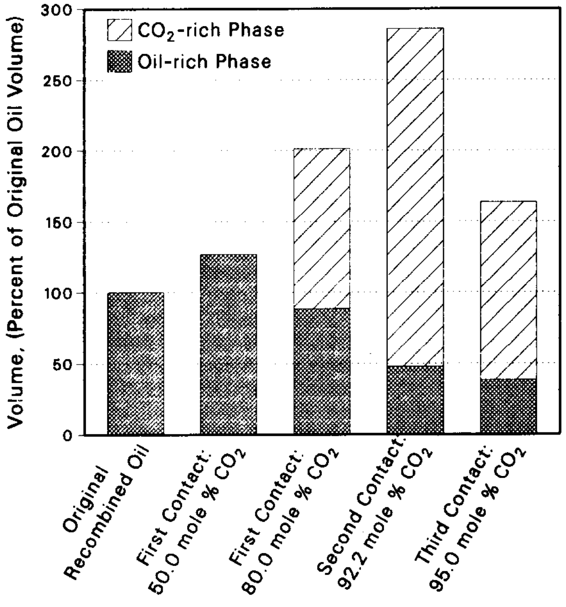

Figure 18 - Phase distributions in Oil C1 - CO_2 system CO_2 cycling study at 94°F and 1615 psia (307.6 K and 11.14 MPa)

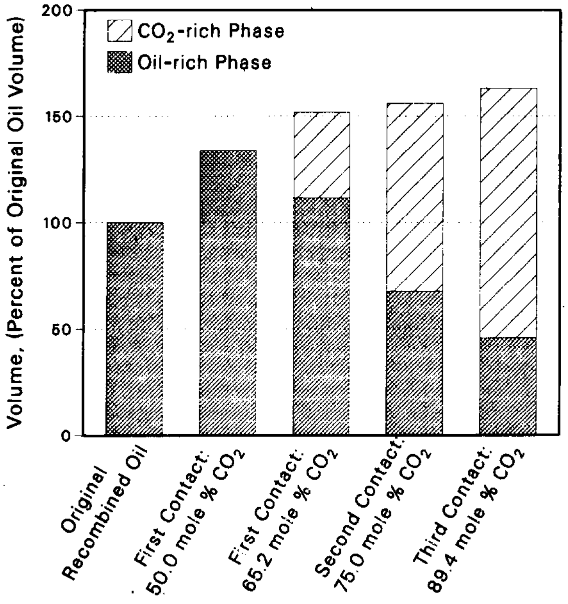

Figure 19 - Phase distributions in Oil F - CO_2 system CO_2 cycling study at 105°F and 2015 psia (313.7 K and 13.89 MPa)

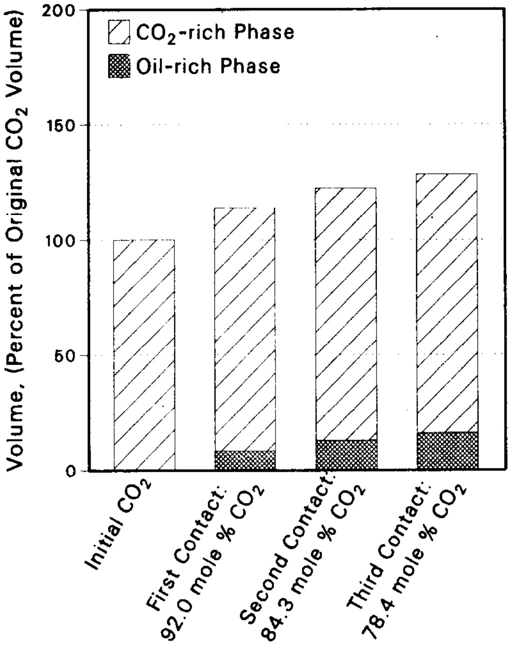

Figure 20 - Phase distributions in Oil A - CO_2 system oil cycling study at 105°F and 2015 psia (313.7 K and 13.89 MPa)

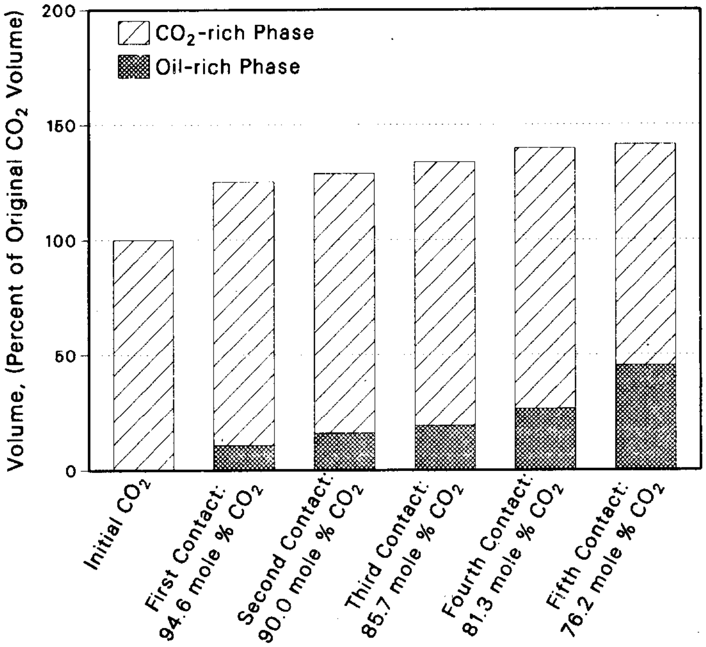

Figure 21 - Phase distributions in Oil B1 - CO_2 system oil cycling study at 106°F and 2015 psia (314.3 K and 13.89 MPa)